GCP/RAF/271/FIN-TD/77 (En) November 1997

THE NOAA SERIES' AVHRR RADIOMETER'S CAPABILITY OF REVEALING WATER FEATLTRES IN LAKE TANGANYIKA

by
V. Tuomainen, H. Mölsä, J. Parkkinen, L. Patomaki
and O.V. Lindqvist

FINNISH INTERNATIONAL DEVELOPMENT AGENCY

FOOD AND AGRICULTURE ORGANIZATION
OF THE UNITED NATIONS

Bujumbura, November 1997

PREFACE

The Research for the Management of the Fisheries on Lake Tanganyika project (LTR) became fully operational in January 1992. It is executed by the Food and Agriculture Organization of the United Nations (FAO) and funded by the Finnish International Development Agency (FINNIDA) and the Arab Gulf Program for the United Nations Development Organization (AGFUND).

LTR’s objective is the determination of the biological basis for fish production on Lake Tanganyika, in order to permit the formulation of a coherent lake-wide fisheries management policy for the four riparian States (Burundi, Tanzania, D.R. of Congo and Zambia).

Particular attention is given to the reinforcement of the skills and physical facilities of the fisheries research units in all four beneficiary countries as well as to the build-up of effective coordination mechanisms to ensure full collaboration between the Governments concerned.

Prof. O.V. LINDQVIST
LTR Scientific Coordinator

Dr. George HANEK
LTR Coordinator

LAKE TANGANYIKA RESEARCH (LTR)
FAO
B.P. 1250
BUJUMBURA
BURUNDI

Telex: FOODAGRI BDI 5092

Tel: (257) 22.97.60

Fax: (257) 22.97.61

e-mail: ltrbdi@cbinf.com

GCP/RAF/271/FIN PUBLICATIONS

Publications of the project are issued in two series:

* a series of **technical documents (GCP/RAF/271/FIN-TD)** related to meetings, missions and research organized by the project;

* a series of **manuals and field guides (GCP/RAF/271/FIN-FM)** related to training and field work activities conducted in the framework of the project.

For both series, reference is further made to the document number **(01),** and the language in which the document is issued: English **(En)** and/or French **(Fr)**.

For bibliographic purposes this document should be cited as follows:

Tuomainen, V., H. Mölsä, J. Parkkinen, L. Patomäki and O.V. Lindqvist, The NOAA series' AVHRR radiometer's capability of reveling water features in Lake Tanganyika. FAO/FINNIDA Research for the Management of the Fisheries of Lake Tanganyika. **GCP/RAF/271/FIN-TD/77 (En): 29p.**
1997

Acknowledgements

We are greatly indebted to the financial assistance of the University of Kuopio and Lappeenranta University of Technology, which made image processing and development of image processing tools possible.

TABLE OF CONTENTS

LIST OF TABLES

LIST OF FIGURES

LIST OF ABBREVIATIONS

ATSR	Along Track Scanning Radiometer
AVHRR	Advanced Very High Resolution Radiometer
ESA	European Space Agency
ERS	European Remote sensing Satellite
GMT	Greenwich Mean Time
HRV	High Resolution Visible
NDVI	Normalized Difference Vegetation Index
NOAA	National Oceanic and Atmospheric Administration
PC	Personal Computer
SPOT	Systéme Probatoire d’Observation de la Terre
TM	Thematic Mapper
USGS	United States Geological Survey
WWW	World Wide Web

1 INTRODUCTION

Remote sensing is used at the Lake Tanganyika Research Project (LTR-Project) to provide information on the spatial and temporal variations of surface water conditions of the lake. In favourable conditions, this method enables data of temperature lake-wide to be obtained, which is not possible by any reasonable field sampling programme. The image analysis calibrated with actual ground-truth measurements, can thus be used in estimating the relative physical and biological differences in and between the surface areas of the lake. Remote sensing gives complementary results directly to the other components of the LTR programme such as limnology and hydrodynamics, and it is hoped, also indirectly to fish biology and plankton ecology.

It is used to observe the occurrence and extent of the expected upwelling events, especially at the southern end of the lake but also in other parts. These observations will first be related to the hydrological model of the lake. We also hope to use the images for areal comparisons between different parts of the lake and relate them to possible differences in its limnology and biological production at large. The two parameters we are employing now are primarily surface temperature and secondarily the so-called vegetation index.

Satellite based remote sensing has been used in environmental research since the early 1970’s. During the past few years, however, its use has been greatly expanded, partly due to the easier accessibility of satellite images than before and to the reduction in price. Furthermore, the imaging characteristics have been greatly developed during the past two decades.

One of the first tasks of this study was to find out the feasibility of different satellite sensors and their channels for the project’s use. The other aims were to set up the routines for analyses of satellite images and, accordingly, to process some sample images of Lake Tanganyika for preliminary investigation of the lake water dynamics.

This report describes some basics of satellite imagery and provides the criteria for selection of NOAA AVHRR images as well as the image analyses of Lake Tanganyika. For the temperature analysis field measurements are used to developed a temperature model. The final part discusses the results.

2 BASICS OF REMOTE SENSING

2.1 Basic aspects

When using a multichannel sensor technique in the space-borne remote sensing, it is possible to measure the earth through several narrow windows, which lie in different parts of the electromagnetic spectrum. Each of these windows usually known as channels (or bands), describes the distribution of the light reflected from the earth's surface or the heat radiated by the earth. On the visible region of the electromagnetic spectrum (370 – 700 nm), the satellite measurement corresponds to the situation where the globe was observed through a coloured filter, whereas the channels located to the far infra red wavelengths (8 – 14 μm) reveal the distribution of the surface temperature. If the spectral properties of phenomena about which information is needed are known, a suitable existing satellite can be chosen for use.

By properly designing the wavelength region for the channels of satellite sensor, the desired information can be obtained. For example, in order to obtain an estimate of chlorophyll *a* concentration, one channel should be around the top of the chlorophyll absorption peak and another (reference) channel on the

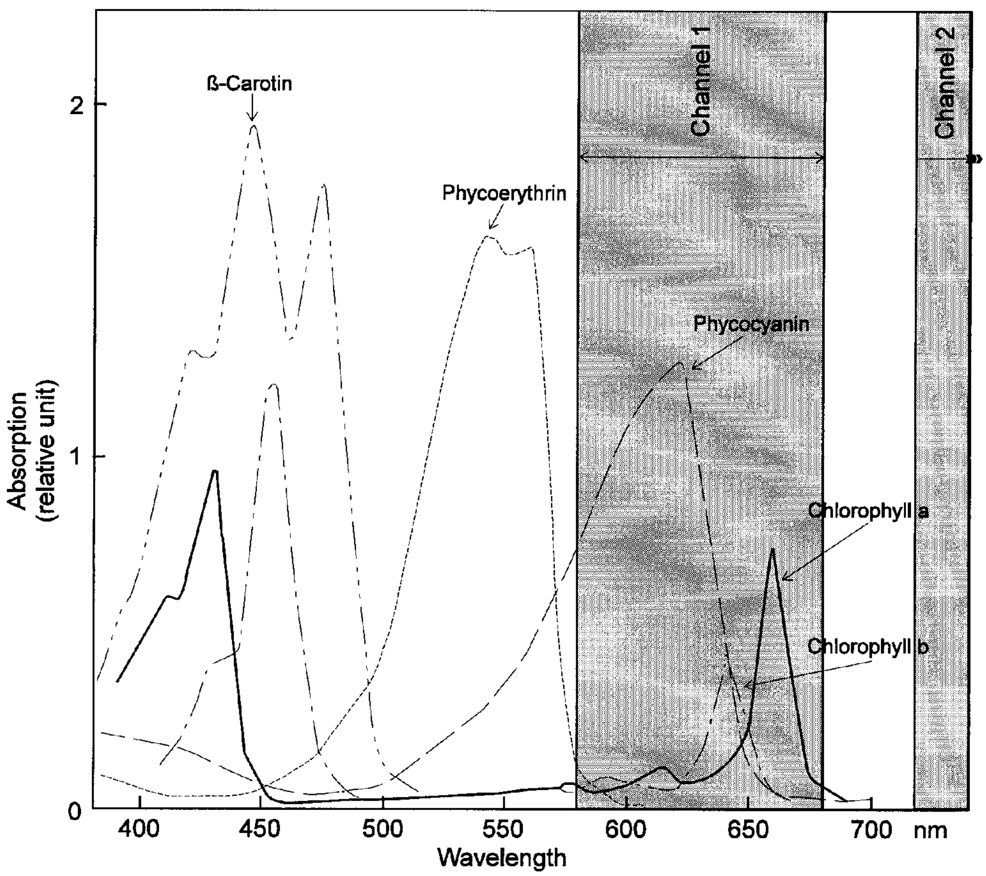

Figure 1. The absorption spectrum of the chlorophyll *a* (Hoppe W, et al., 1978), and the NOAA AVHRR channels covering that spectral region.

wavelength region where chlorophyll *a* has no effect. From Figure 1, one can see that the channel at 400 – 450 nm or 650 – 680 nm could be the first channel and the other channel could be located anywhere from 450 nm to 600 nm or above 700 nm. In case of the AVHRR sensor of NOAA satellites the spectral channels cannot be chosen by will. Instead they are fixed with only one channel being within the visible region of the electromagnetic spectrum as shown in Figure 1. This channel covers a much larger region than necessary for chlorophyll *a* and thus may include information from other sources as well. However, the most probable source is vegetation. Therefore all information from these measurements is referred to as indicating “vegetation” instead of chlorophyll *a*.

2.2 Satellite alternatives

At the beginning of the Lake Tanganyika Research Project four of the present earth-orbiting satellite series could be considered, namely NOAA, ERS, Landsat, and SPOT. Some general characteristics of the AVHRR sensor of NOAA series satellite are shown in Table 1.

One of the sensors (ATSR) inboard in ERS-l satellite has thermal channels almost similar to AVHRR, but no channels at the visible region of the electromagnetic spectrum. At the beginning of 1996 ESA launched another satellite, named ERS-2, which is bundled with more advanced sensors adding the possibility to acquire data at three different visible regions of the electromagnetic spectrum. In the TM sensor of Landsat satellite there are six channels: three at the visible and three at the infrared (one thermal) wavelength of the electromagnetic spectrum. The HRV sensor (in multispectral mode) mounted to the SPOT satellite has only three visible channels. The sensors of the Landsat and SPOT series satellites would provide 8-bit radiometric resolution much better and spectral resolution slightly better than the NOAA series whose sensor has 10-bit radiometric resolution.

The scene area of the AVHRR sensor is 3000 km x 6000 km and there are always two functional satellites at the orbit. Therefore it is possible to get useful satellite data on a certain location on the ground at four different times of the day. In the case of the TM or HRV sensor, one scene area of 185 km x 170 km, 60 km x 60 km, respectively, does not cover the whole lake. Hence, several scenes must be used with the result that the whole lake could not be imaged on the same day. It should also be noted that the revisit intervals are 16 and 26 days for the Landsat and SPOT satellites, respectively. An additional drawback with the Landsat and SPOT data is that they are much too expensive for the current budget of the LTR-project. The lowest price of one AVHRR data scene is $50, but the prices of satellite data varies greatly with the distribution site (and a post-processing state of a product). The EROS data center provided the least expensive Landsat data full scene at $425, but prices can range to up to $5000. The data from other satellites are also much more expensive than that of the AVHRR. The spatial resolution of the AVHRR sensor (1.1km x 1.1km) NOAA satellite’s is not very good when compared to that of the TM
(30 m x 30 m in visible and near-IR, 120 m x 120 m in thermal IR) of the Landsat or the HRV sensor (20 m x 20 m) of SPOT. Lake

Table 1. The characteristics of AVHRR radiometer.

Channel number	*Wavelength (μm)*	*Spectral category*
1	0.58 - 0.68	green - red
2	0.725 - 1.10	near IR
3	3.55 - 3.93	middle IR
4	10.3 - 11.3	thermal IR
5	11.5 - 12.5	thermal IR

Tanganyika is, however, so large in its area and lacks complicated shore lines and small islands so that the AVHRR resolution might be good enough for the task. Taking into consideration all the above aspects the NOAA satellite was chosen for the project.

For further reference on the basis of remote sensing as well as the characteristics of the different satellites one should consult, e.g., Colwell R. N. (1983), Jensen J. R. (1986), Lillesand & Kiefer (1987), Mather P. M. (1987), and Meaden & Kapetsky (1991). The latest information about the above and other existing satellites could be found e.g. at the Internet address http://www.geog.nott.ac.uk/remote/satfaq.html.

During this project data from the Russian Resurs-Ol satellite series has been made available by Eurimage (http://www.eurimage.it). The satellite carries the MSU-SK multispectral scanner, which has four channels in visible and near-IR region of the electromagnetic spectrum with a 160 m spatial resolution, and one channel in thermal IR region with a 600 m spatial resolution. The data is acquired at 8-bit resolution with the revisit time of 4 days at the equator, and it covers the area of 600 km x 600 km for each scene at the price of approximately $1800. In the near future one of the most promising satellites for large scale vegetation study is mounted in a SeaStar spacecraft. It was launch in August 1997 carrying the SeaWIFS instrument, which has eight narrow (20 – 40 nm) spectral channels centered at 412, 443, 490, 510, *555,* 670, 765, and 865 nm with a 10-bit radiometric resolution. From a 705 km orbital altitude the satellite acquires data with a maximum scan angle of 58.3° and a 1.13 km spatial resolution at the nadir. The swath width could be estimated comparing the technical data of AVHRR: a scan angle of 55.4° and a 1.1 km spatial resolution at the nadir. Further information about this satellite can be found at *http://seawifs.gsfc.nasa.gov/scripts/SEAWIFS.html.*

2.3 Sources of images

The data from the AVHRR sensor of the NOAA satellite, which covers the Lake Tanganyika area, may be obtained from at least four commercial sources:

1. Eurimage in Frascati (Rome), Italy, cooperating with the European Space Agency
   (ESA);
2. Satellite Applications Centre in Pretoria, South Africa;
3. EROS data center (USGS), which stores also satellite data

received from South Africa, La Reunion and Nairobi;
4. Satellite active archive (SAA) of NOAA.

In addition to these above mentioned commercial sources, the UK/SADC Lake Fisheries Project on Lake Malawi is receiving the AVHRR data with its own receiver.

All of the 1993 data and two batches of 1994 data from the AVHRR sensor for the LTR Project were purchased from the Eurimage via the Satellite Image Centre of National Land Survey of Finland. The rest of the 1994 and all of the 1995 data have been purchased from the EROS data center.

A comprehensive starting point to survey various satellite data sources (including most of the above discussed) and other subjects relating to remote sensing can be found from the WWW virtual library of remote sensing at
http://www.vtt.fi/aut/rs/virtual/

3 SATELLITE IMAGE ANALYSIS

3.1 Geometric rectification and image remapping

The sources of geometric distortions include instrument error, panoramic distortion, earth rotation and platform instability (Mather, 1987). When an image is constructed from the satellite data, these errors affect the quality of the image. One of the most obvious instrument errors is-an erroneous scan line, which is seen as a well-defined stripe in the constructed image. In the case of fixed optics using wide viewing sensors (like AVHHR), when data is obtained from a considerably larger area than at the nadir, panoramic distortion is introduced with the measurement geometry doing the most at the extreme angles of the measurement. So the accuracy of the image decreases towards the edges of the scan line and the information from one ground location (or part of it) could be effecting several scan points. The distortion induced by the rotation of the earth skews the image and the variations in altitude or attitude of the satellite, produces further inaccuracy to the image.

It is essential for the model development that the same geographic location (longitude, latitude) can be found from the ground surface measurement and the satellite data. If the position of the satellite data needs to be rectified geometrically, as in the case of AVHRR, one possible solution is to fit the locations of some well seen earth features, ground control points (GCP's), to their counterparts in a satellite image, and another is to calculate geographic coordinates of the satellite data from the parameters described by orbital geometry model of the satellite. If the first method is chosen, a sufficient amount of points must be identified from the satellite image and from a geographic map of that same area. Then the transformation equation must be determined using least-squares criteria, so that given image coordinates, geographic coordinates can be calculated as accurately as possible. With the second method the distortions are corrected mathematically using the knowledge of the measuring instrument (e.g. the speed of the rotating mirror) and the orbital characteristics of the satellite: altitude, attitude, inclination angle, speed, and date is needed.

After the transformation equation between ground control points to image points is determined, any value of the image can be assigned to a unique geographic point. If we are going to visualise the satellite data in a map projection, an equally spaced grid is required. In general this is not valid for the satellite data, thus the values of a new grid must be determined from unequally spaced satellite data. The easiest way is to find the nearest satellite data point for each grid points and give the value of this point to the grid point. This method is often called the nearest neighbour interpolation. Other methods used to map a grid are more complicated and more often than not use averaging of surrounding values with or without distance based weights. The first method is computationally superior in its efficiency. A further advantage is that it does not alter mapped values. Occasionally there is a drawback for the interpreter of the data that low scale phenomena hide larger scale patterns from view

3.2 Vegetation index

In the optimal case, the satellite image analysis should be based on the spectral characteristics of the ground target. The amount of chlorophyll *a* in one spot of an image could be estimated from a satellite based measurement so that

(1) $\text{chl } a = c_1 + c_2 R,$

where c_1 and c_2 are constants and R is upwelling radiance. From Figure 1 it could be seen that chlorophyll *a* absorbs incoming radiation in two rather narrow channels centered at 440 and 670 nm. One widely used method in the satellite remote sensing is that instead of measuring in a single wavelength, the ratio of radiances from two different wavelengths are utilised so that one channel is located in the spectral region where absorption occurs and another where it does not. The most reliable results have been obtained using the 440/550 nm or 520/550 nm ratio of radiances from the Coastal Zone Color Scanner, Kirk (1983).

In the case of the NOAA satellites' AVHRR sensor, the above equation does not necessarily give reliable results due to the improper spectral channels available. The channel with which the amount of chlorophyll *a* should be measured is too wide to give proper radiance values for the use of above equation. So, another equation is introduced to give a rough estimate of the vegetation in the measurement area

(2) $$NDVI = \frac{CH_2 - CH_1}{CH_2 + CH_1},$$

where NDVI is the so called "normalized difference vegetation index", and where CH_1 is the raw 10 bit measured data of the channel i (Los, 1993). Here channel 1 includes one absorption peak of chlorophyll *a* and channel 2 as a reference channel does not.

The previous equation can be modified knowing the technical characteristics of the measurement instrument. So reflectance R (or radiance) values can be determined from the raw data using the calibration tables from NOAA (Los, 1993) for each channel i. Now the index could be expressed as

(3) $$NDVI = \frac{R_2 - R_1}{R_2 + R_1},$$

Further enhancement could be achieved by decreasing the lowest value of the data in each channel, Chavez (1988). This is effectively one kind of atmospheric correction and is based on the idea that the radiance at least in one data point in every measurement on visible or near-IR channel is equal to zero and thus the non-zero value in that point indicates the contribution of the atmosphere. This method is far from reliable since it is sometimes difficult to be sure that the lowest value is not an erroneous one. Furthermore, this method gives only relative values of the NDVI. But the advantage of this simple first degree atmospheric correction is that it does not need any other than satellite derived data. There are a number of sophisticated atmospheric correction methods, but most of them need extra information from atmospheric condition, Jensen (1986). For this reason we have not attempted to use them.

3.3 Lake surface temperature

At the moment the most important attribute computed from the satellite data is the lake surface temperature. As stated before, this can be determined directly from a thermal channel measurement. In the case of the AVHRR sensor, there are two thermal channels (channels 4 and 5), whose data can be used to determine temperature at any time of day.

When computing the actual temperature, it is important to know the functional dependence between surface temperature and surface radiance. For the AVHRR sensor this dependence is almost linear for both of the two thermal channels. At the satellite measured radiance *(L)* of each channel is first converted to a 10-bit integer value *(N)* and then stored digitally on board. The measured radiance can be restored from digital values knowing the conversion parameters, the slope (g) and the intercept *(o)* used with the equation

(4) $L_i = g_i N_i + o_i$,

where i denotes channels 4 or 5. It should be noted that the slope and the intercept are not the same throughout the measured scene, but vary with each scan line (the mirror of measuring instrument rotates once from an extreme left to right position) based on the onboard calibration of reference temperature sources. Once the radiance has been solved and the spectral response function of the channel is known, the radiance can be related to the temperature by the following equation, Planet (1988),

(5) $L(T) = \int_{v_1}^{v_n} B(v,T)W(v)dv,$

where *W* is a normalised response function of a channel, v_1 and v_n are the radiation frequencies at the beginning and end of the channel and *B* is the classical Planckian function for blackbody radiation

$$B(v,T) = \frac{2hc^2v^3}{e^{hv/kT} - 1},$$

where h is Planck's constant, c is the speed of light, k is Bolzmann's constant and *T* is the temperature. When the function *W* is known for a channel, values of *L* at different temperatures *T* can be calculated given thus numerically the function *L=L(T).* This may be tabulated and inverted to give *T=T(L),* i.e., temperature as a function of *L.*

In theory the temperature could be correctly computed from the data of either of the two channels using the above equations. In a real life situation there is always an atmospheric layer present, in which radiation is affected by scattering and absorption, when the satellite is measuring radiation above the surface of the earth. In order to get better estimates of the temperature on the surface of the earth in these conditions, the split window method (Anding and Kauth, 1970) has been introduced. In this method data from both of the two thermal channels *(T_4 and T_5)* is used to estimate surface temperature (T_s) according to the following equation

(6) $T_s = K_0 + k_1 T_4 + k_2 (T_4 - T_5),$

where parameters k~ can be determined from least squares solution of the equation for each i (0,1 and 2). The main idea in the above equation is, that the difference of the thermal channels is utilised to compensate the effect of the atmosphere (especially water vapour), because the channels are located in the different spectral region. To speed up the computation of the temperature, above equation could be modified to the following form

(7) $T_s = a_0 + a_1 T_4 + a_2 T_5.$

It should be noted that the parameters in this equation are not the same as in the previous one, but they can be easily converted if required. With the above equation the path length of the thermal radiation through an atmospheric layer is omitted. If the path length of the radiation is took into consideration, the equation

(8) $T_s = k_0 + k_1 T_4 + k_2 (T_4 - T_5) + k_3 (T_4 - T_5)(\sec(\phi) - 1)$

where ϕ is the satellite zenith angle, Kidwell (1995), must be used instead of (6) or (7).

4 RESULTS

4.1 Satellite data and processing scheme

For calibrating the satellite data to correspond to conditions on the earth's surface, ground truth data is needed. The satellite data must meet two basic criteria, before a ground measurement can be referenced to it. The first is that there is prevailing a clear sky condition in a reference area and the second is that the ground measurement is done concurrently with the satellite overpass.

An image, which spatial resolution is reduced, is known as a quick-look image. From these kind of images it is possible to validate the quality of the satellite data.

At first there were temperature measurement data from a buoy in the Kasaba bay, which is located in the southern part of Lake Tanganyika, off Mpulungu, from 1993 to 1994. Before ordering actual NOAA AVHRR satellite data at that time, several quick-look images were ordered from the Eurimage. After careful study the buoy seemed to be in a cloudless area in fourteen of these images, so corresponding satellite data was ordered from the Image Centre of National Land Survey of Finland, which is a local agent of the Eurimage. The satellite data was delivered in SHARP-2A-format.

Certain radiometric processing of satellite data has been done in the SHARP-2A-format. Data from the first two channels of the AVHRR instrument have been processed from radiance based digital numbers to equivalent reflectance so that the illumination angle has been set to 900 in every location of the image. The reflectance values can vary from 0 to 100 percent. The last two channels of satellite data have been processed from radiance based digital numbers to brightness temperature, taking into consideration the nonlinear behaviour of each channel response function.

In addition to the radiometric processing of data, there are a few additional features in SHARP-2A-formatted data. For example, some classification algorithms have been used to separate land masses from water bodies and to identify clouds. The most important of these features is the geometric registration of the satellite image. Further details can be found in the technical specification of format (SHARP-2A, 1992) and in the user guide (SHARP LEVEL 2, 1992).

Later data from another buoy, which is located in the northern part of the lake near Kigoma, became available for use as well as 1995 data from both buoys. So more satellite data were needed. After inquiring to Eurimage, it was found, that they had no recent data available, so another place needed to be found. The EROS data center has an online data service, which can be reached by anyone connected to the Internet. There it is possible to study quick-look images from NOAA AVHRR satellites at almost real time and an archive from previously acquired data extends to year 1995. So this service seemed to be ideal for our purposes. Keeping in mind the basic criteria for the data in the case of both buoys, 1994 and 1995 quick-look images were carefully examined yielding to an order of 28 satellite data files. The files were delivered in a Level- lB-format. A detailed description of this format can be found from Kidwell, 1995.

A UNIX-workstation (Silicon Graphics Crimson) has been used mainly to process satellite data with a help of two kinds of software. One of them is commercial and the other is freely available, named MATLAB and Generic Mapping Tools (Wessel P., 1991, Wessel P., 1995), respectively. Because the first one is designed for mathematical computation, it was suitable for most tasks in the processing scheme. The second software is suitable for the post-processing of images like transferring them from geographic coordinates to various map projections. In addition to the workstation some tasks were accomplished with PC using Linux and Windows.

4.2 Additional information on the cloudiness of Lake Tanganyika

After receiving the first satellite data from the AVHRR, it was noticed that preliminary knowledge of cloudiness over Lake Tanganyika could be attained from Meteosat satellite data. Meteosat satellite is a geostationary satellite orbiting the earth at an altitude of 36000 km above the equator at a speed which keeps it at the same position with respect to the earth. From this position 42 % of the globe including Africa is imaged every 30 minutes in three spectral regions. After acquisition, satellite data is received and processed at Nottingham University so that cloud cover of the earth can been seen from these processed images. Although the images are stored at a reduced quality, at the beginning of 1995 a routine was developed to obtain daily Meteosat satellite images in Kuopio from Nottingham University through the Internet.

To predict the cloudiness over Lake Tanganyika a subjective classification scheme was introduced. The classification groups were selected so that in cloudy or very cloudy conditions it is not possible to obtain any information of the lake from satellite data in the visible or infrared region of the electromagnetic spectrum. In moderate conditions there is a fair possibility of obtaining useful information at least of those parts of the lake, where the measurement buoys are located. In clear conditions the whole lake is seen clearly from the satellite giving the best possibilities to interpret the data. This kind of subjective study of cloudiness in 1995 is given in Table 2.

Table 2. A subjective categorisation of cloudiness over Lake Tanganyika in 1995 based on Meteosat images.

month	*cloudy or very cloudy*	*moderate*	*clear*
1	1–14, 16–25, 27–31	15, 26	
2	1, 4–17, 19–27	2–3, 18, 28	
3	3, 5–13, 15–16, 22–31	1–2, 4, 14, 17–20	
4	6–8, 10–12, 22–28	3–5, 9, 13–16, 18–21, 29–30	1–2, 17
5	5, 7, 10, 28–29	1–4, 6, 8–9, 11, 13–19, 25–27, 30–31	12, 20–24
6	2–7	1, 8–9, 15–22, 29–30	10–14, 23–28
7		2, 6–15, 18–19, 23–24, 26–31	1, 3–5, 16–17, 20–22, 25
8		1, 5–7, 13–14, 16, 20–21, 23, 28–29	2–4, 8–12, 15, 17–19, 22, 24–27, 30–31
9	11–12, 26–28, 30	3–6, 8–10, 13–15, 17–20, 25, 29	1–2, 7, 16, 21–24
10	2, 4–6, 12–13, 15–16, 18–21, 25–29	1, 3, 7–11, 14, 17, 22–23, 30–31	
11	3, 7–8, 10, 13, 17–30	1–2, 4–6, 9, 11–12, 14–16	
12	1, 5–6, 8–10, 13–31	2–4, 7, 11–12	

4.3 Vegetation index and surface temperature

It was common practice with all AVHRR data to first carry out the process to remove geometric distortions. In the processing scheme geographic control points (GCP' s) were fitted to their counterparts in image points in such a way that the fitting error was minimised. Two different processing method had to be utilised because of the differences in the data formats. First, the geographic area to be used for control points was selected. Best fit between GCP's and image were sought separately for each scan line in the Level-lB-format images. For SHARP-2A-format images, the fit was done at the same time to all GCP's in the area, since GCP's for each scan line are not available. The GCP' s discussed above are included in the satellite data and are calculated onboard based on the satellite's clock. But as the clock is known to drift, at this stage only the systematic rectification was gained. So the linear error still remained in geographic coordinates. Finally, selecting corresponding coordinates of well shown features from CIA World Data Bank II (bundled with Generic Mapping Tools) and from the satellite image, the satellite data was shifted to the right position. After determining the vegetation index or surface temperature, the data was remapped to a Cassini cylindrical projection using the nearest neighbour interpolation method.

Because the chlorophyll *a* concentration was zero at the surface of the lake according to Huttula (1997), satellite data was not attempted to relate to it using the equation (1). Instead images describing the vegetation index was determined according to the equation (3) for all AVHRR data mainly for demonstrative purposes. Two of the processed images are presented in Figure 3 and Figure 4.

The measurements of the thermal channels of the satellite were used in conjunction with the earth based reference data to determine the parameters of the equation (6). After that the lake surface temperature could be estimated based on that very equation.

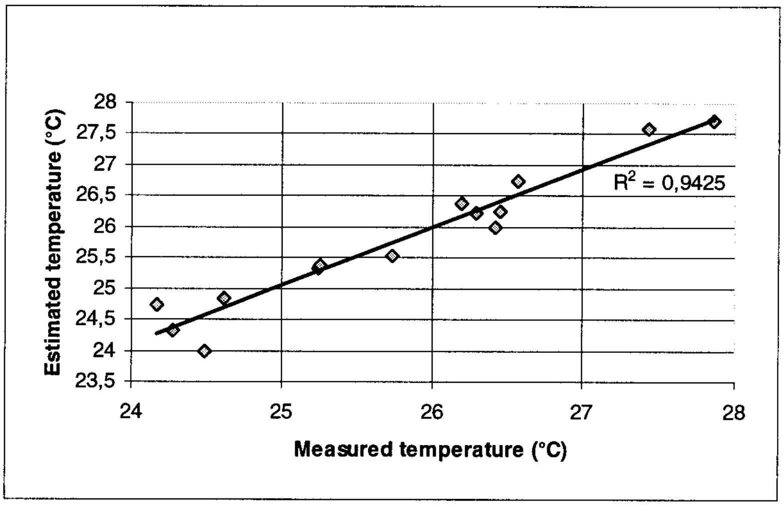

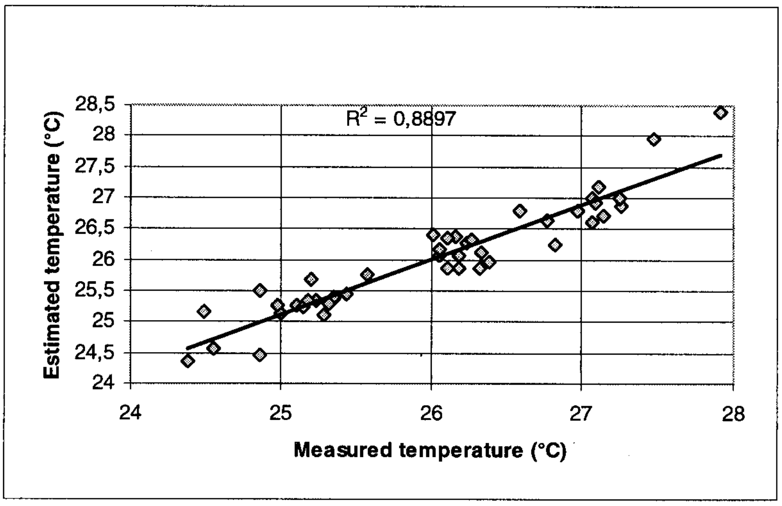

Figure 2. Temperature dependencies between measured buoy and estimated satellite temperatures for NOAA-11 and NOAA-14 satellites (upper and lower, respectively).

Table 3. Fitted parameters in equation (7) according to our work and literature.

Authors	a_0	a_1	a_2	Standard Error (K)	R^2
McMillan & Crosby (1984)	-0.5820	3.7020	-2.7020	0.8039	
McClain *et. al.* (1985)	4.7400	3.6540	-2.6680	1.1382	
Yokoyama and Tanaba (1991)	0.5300	3.3310	-2.3310	0.6311	
Wooster *et. al.* (1994)	6.9800	3.1961	-2.2130	0.54	0.84
Our work, NOAA-11	5.3379	2.3348	-1.5155	0.3016	0.94
Our work, NOAA-14	3.3780	2.9946	-2.1719	0.3056	0.89

As stated before there are two different measurement buoys on Lake Tanganyika, one near Kigoma and another off Mpulungu. These buoys have temperature measurement chains so that one instrument is located at 2.6 m above surface and several other instruments below the surface of the lake. The highest and the lowest are a the depths of 1 m and 300 m, respectively. To estimate lake temperature based on NOAA-l1 satellite data, fourteen data files from May 1993 to May 1994 were used. Because there were ground measurements only from the buoy off Mpulungu, the satellite data files were inspected only at that location. All the files met selection criteria and were used in linear regression analysis. In the case of the NOAA-14 satellite 28 data files from February to September 1995 were used. On the dates of these data files, there were measurement from both buoys. From 56 possible reference points 45 were chosen for regression analysis. Because the temperature data from the buoys was registered at 30 and 60 minutes intervals from Kigoma and Mpulungu, respectively, it was first linearly fitted to the time of the satellite measurement of that same area before using it in the regression analysis. The data at the depth of 1 m alone was chosen to represent the surface temperature. In Figure 2 buoy temperatures are plotted against estimated satellite temperatures, separately for NOAA-11 and -14 data. In addition the regression line has been drawn. The essential results from regressions (Eq. 7) along with some other previously published results can be seen from Table 3. Here it should be noted that Wooster et. al. have fitted their parameters with night-time satellite measurements.

Finally, all AVHRR data were processed to temperature images according to equation 7. A few temperature images are presented in Figure *5* -— Figure 13.

5 DISCUSSION

Remote sensing was chosen as one of the components of the project based on the assumption that it is able to reveal some essential water quality parameters contemporaneously for the entire lake, which is not possible with any other method. Based on the knowledge of other work done with the NOAA-AVHRR instrument, it was obvious at the beginning, that the surface temperature could be estimated with good accuracy for the lake as soon as there were adequate temperature measurements to calibrate satellite data. In addition it was hoped that the relation between satellite data and the concentration of the chlorophyll at the surface of the water could be solved.

In order to develop a model for the water quality parameters, it is a common practice for satellite data to be verified to the corresponding measurement on the ground. So this kind of approach was chosen here also.

According to Nakayama (1994) it was thought that the concentration of the chlorophyll could be related to the satellite data. Further encouraging expectations arose from Kirk (1983) specifying that the fluorescence peak of algal cells was at about 685 nm, which could be detected with the AVHRR radiometer (see Table 1 and Figure 7.7, Kirk). Soon this work was discontinued, because it was observed that the concentration vanished early in the morning, Huttula (1997). But it should be noticed, that the data from the visible and near-IR channels of the satellite reveal some other water features, which are not known so far. For example, in Figure 3 it could be seen that the mouth estuary of the Malagarasi river is responsible for the diminishing NDVI values across the lake. In Figure 4 this phenomenon is distinctly observed, but now the influence is restricted to a smaller area. One should be aware when interpreting this image more closely, that values greater than -0.40 should be considered erroneous due to presence of different kind of clouds.

As for the temperature, the local temperature model developed for the daytime satellite measurement in this study seems to give a good estimate of the temperature for both satellites, NOAA-11 and -14, as one could verify from the results introduced in Figure 2 and in Table 3. Furthermore, there are three clear temperature patterns in these temperature images: annual, locally cumulated temperature areas, changes of temperature in the mouth estuary of Malagarasi river, and cooling (warming) of water masses in successive days. The first phenomenon could be observed in Figure 5, Figure 6, and Figure 7, and could be due to seasonal change of climate: cool, dry season is changing to hot, dry season. The second phenomenon could be also related to seasonal variation. The mouth estuary of Malagarasi river is cooler than the rest of the water in that same area from the end of May to the beginning of September and warmer at other time. The warm, wet season is reported to change to cool, dry season somewhere between April to May. In Figure 8 – Figure 13 the mouth estuary of Malagarasi river was observed as being cooler. Furthermore, the colder water, initially at the southern part of the lake, is moving towards north.

6 Conclusion

It has been shown in this study that data from two of the thermal channels of the AVHRR radiometer of the NOAA series satellites can reveal the contemporaneous, horizontal surface temperature for the whole Lake Tanganyika with good accuracy both in space and time. Furthermore, cumulated temperatures with various size in area were detected, and upwelling events have also been identified by Huttula (1997). The third thermal channel claims to enhance the accuracy of the surface temperature during nighttime, but this assumption could not be verified, because of a lack of an adequate amount of satellite data.

The data from any channel of the AVHRR radiometer of the NOAA series satellites could not be used to estimate the concentration of the chlorophyll in Lake Tanganyika. This is because the satellite measures the water column only at the thin surface of the lake, where Huttula *et al*. have noticed that based on the fluorescence measurement in the daytime the concentration of the chlorophyll is zero in that water column.

REFERENCES

Anding D. and R. Kauth, 1970. Estimation of sea-surface temperature from space. Remote Sensing of Environment, 1, 217 – 220.

Chavez P. S., Jr., 1988. An improved dark-object substraction technique for atmospheric scattering correction of multispectral data. Remote Sensing of Environment, 24, 459 – 479.

Colwell R.N., ed., 1983. Manual of Remote Sensing (2nd Ed.). American Society of Photogrammetry and Remote Sensing, Falls Church, Va.

Hoppe W., Lohmann W., Marki H., and Zieger H., 1978. Biophysik, em Lehrbuch. Springer Verlag, Berlin.

Huttula T & Podsetchine V., 1997. Hydrodynamics of Lake Tanganyika. Manuscript.

Jensen J. R., 1986. Introductory Digital Image Processing. Prentice-Hall, Eaglewood Cliffs, New Jersey.

Kidwell K.B., ed., 1995. NOAA POLAR ORBITER DATA. USERS GUIDE (TIROSN, NOAA-6, NOAA-7, NOAA-8, NOAA-9, NOAA-l0, NOAA-11, NOAA12, NOAA-13, AND NOAA-14). U.S. DEPARTMENT OF COMMERCE. NOAA/NESDIS/NCDC/SDSC. Washington, D.C.

Lillesand TM. and R.W. Kiefer, 1987. Remote Sensing and Image Interpretation (2nd Ed.). John Wiley & Sons, 721p.

Los S.O., 1993. Calibration adjustment of the NOAA AVHRR Normalized Difference Vegetation Index without recourse to component channel 1 and 2 data. International Journal of Remote Sensing, vol. 14, no. 10.

McClain E. P., Pichel W. G., and C. C. Walton, 1985. Comparative performance of AVHRR based multi-channel sea surface temperatures. Journal of Geophysical Research, 86, 11587 – 11601.

McMillan L. M. and D. S. Crosby, 1984. Theory and Validation of the Multiple Window Sea Surface Temperature Technique. Journal of Geophysical Research, vol. 89, no. C3, pp 3655 – 3661.

Mather P. M., 1987. Computer processing of remotely sensed images: an introduction. John Wiley & Sons, Chicester.

Meaden, G.J. and J.M. Kapetsky, 1991. Geographical information systems and remote sensing in inland fisheries and aquaculture. FAO Fishery Technical Paper 318, FAO, Rome (En): 262p.

Nakayama M., 1994. Application of satellite remote sensing to estimate lake water quality. Mitt. Internat. Verein. Limnol., 24: 345 – 347.

SHARP-2, 1992. Technical Specification of Format. RELEASE 1.0. European Space Agency - Earthnet Programme Office.

SHARP LEVEL-2, 1992. USER GUIDE. Release 1.0. Earthnet Programme Office.

Wessel P., and W. H. F. Smith, 1991. Free software helps map and display data. EOS Trans. Amer. Geophys. U., vol. 72, pp. 441, 445 – 446.

Wessel P.,and W. H. F. Smith, 1995. New version of the Generic Mapping Tools Released. BOS Trans. Amer. Geophys. U., vol. 76, p. 329.

Wooster M. J., Sear C. B., Patterson G., and J. Haigh, 1994. Tropical lake surface temperatures from locally received NOAA- 11 AVHRR data – comparison with in situ measurements. International Journal of Remote Sensing, vol. 15, no. 1.

Yokoyama R., and S. Tanaba, 1991. Estimation of sea surface temperature via AVHRR of NOAA-9 – comparison with fixed buoy data. International Journal of Remote Sensing, 12, 2153 - 2528.

NOAA-11 AVHRR: NDVI

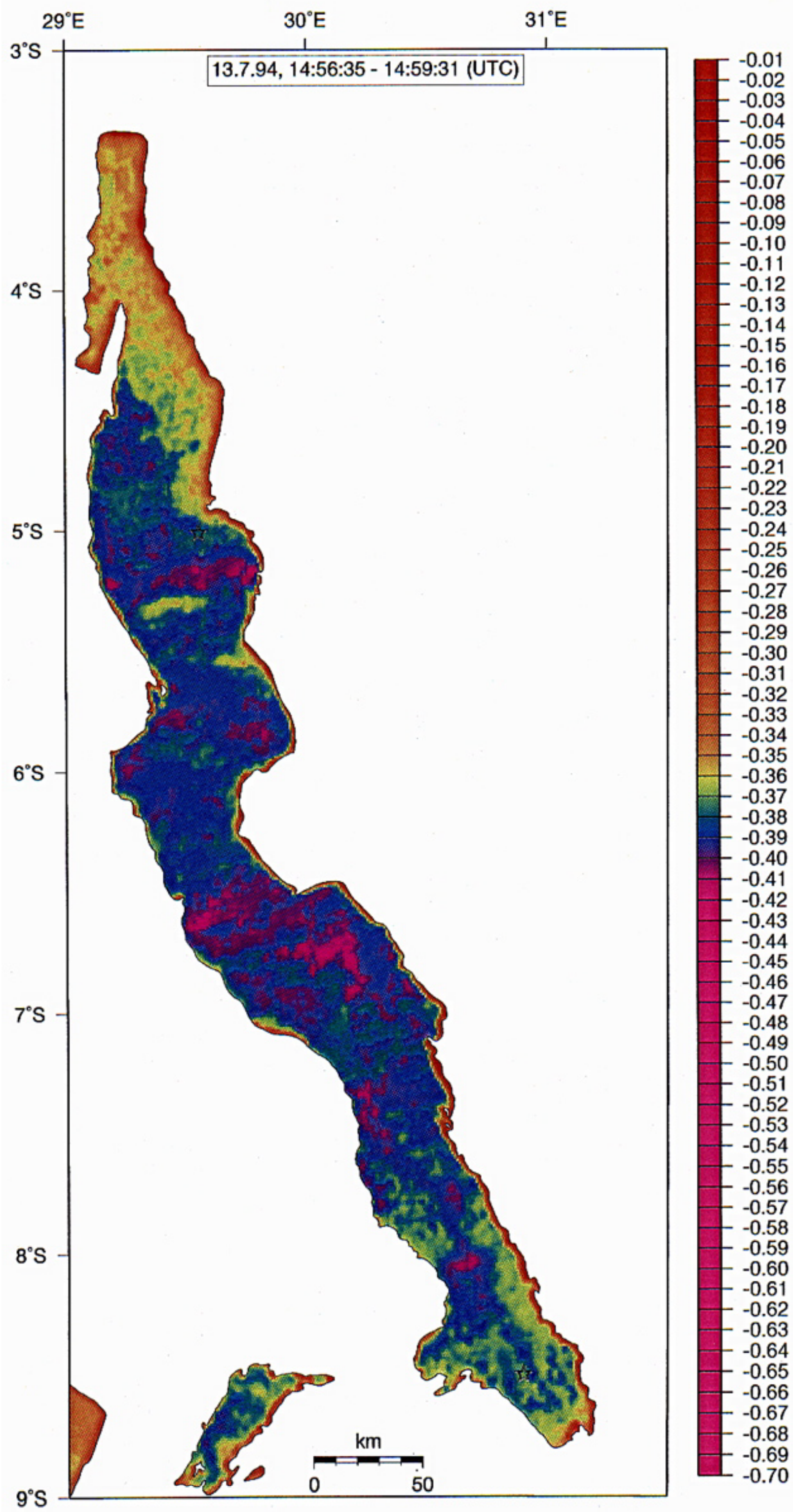

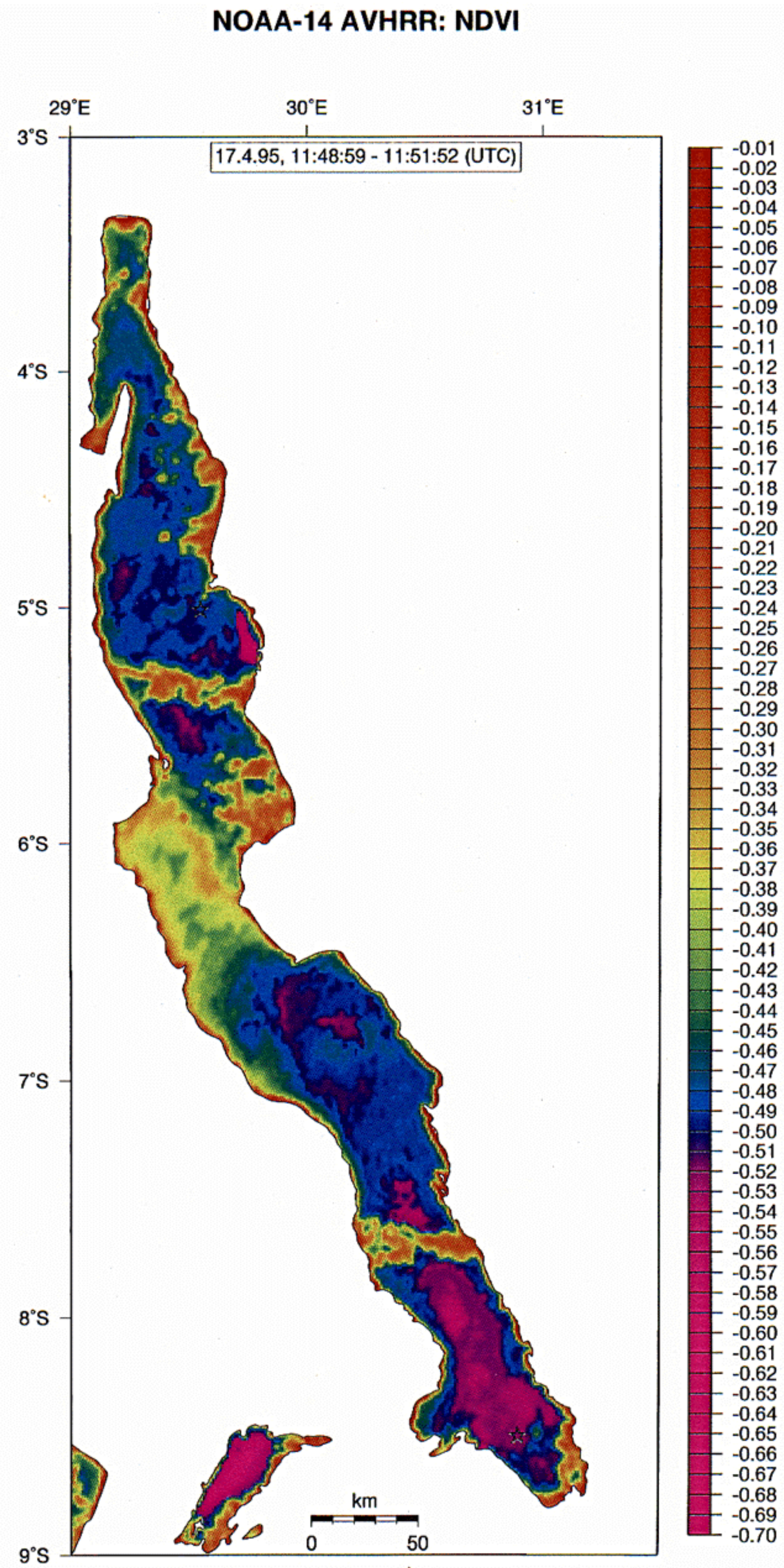
NOAA-14 AVHRR: NDVI
29°E
30°E
31°E
3°S
4°S
5°S
6°S
7°S
8°S
9°S
17.4.95, 11:48:59 - 11:51:52 (UTC)
km
0
50
-0.01
-0.02
-0.03
-0.04
-0.05
-0.06
-0.07
-0.08
-0.09
-0.10
-0.11
-0.12
-0.13
-0.14
-0.15
-0.16
-0.17
-0.18
-0.19
-0.20
-0.21
-0.22
-0.23
-0.24
-0.25
-0.26
-0.27
-0.28
-0.29
-0.30
-0.31
-0.32
-0.33
-0.34
-0.35
-0.36
-0.37
-0.38
-0.39
-0.40
-0.41
-0.42
-0.43
-0.44
-0.45
-0.46
-0.47
-0.48
-0.49
-0.50
-0.51
-0.52
-0.53
-0.54
-0.55
-0.56
-0.57
-0.58
-0.59
-0.60
-0.61
-0.62
-0.63
-0.64
-0.65
-0.66
-0.67
-0.68
-0.69
-0.70

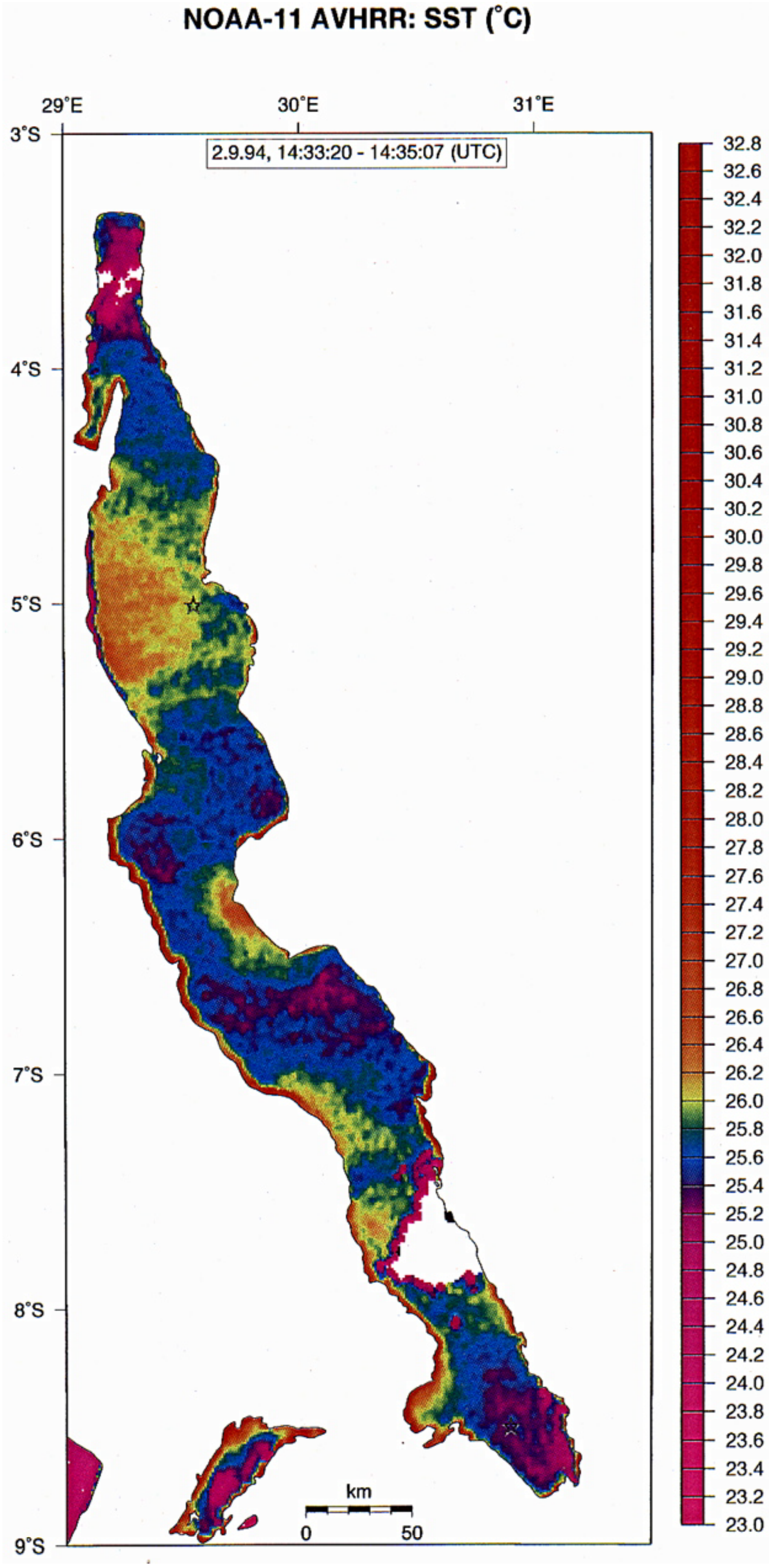
NOAA-11 AVHRR: SST (°C)
2.9.94, 14:33:20 - 14:35:07 (UTC)
29°E
30°E
31°E
3°S
4°S
5°S
6°S
7°S
8°S
9°S
km
0
50
32.8
32.6
32.4
32.2
32.0
31.8
31.6
31.4
31.2
31.0
30.8
30.6
30.4
30.2
30.0
29.8
29.6
29.4
29.2
29.0
28.8
28.6
28.4
28.2
28.0
27.8
27.6
27.4
27.2
27.0
26.8
26.6
26.4
26.2
26.0
25.8
25.6
25.4
25.2
25.0
24.8
24.6
24.4
24.2
24.0
23.8
23.6
23.4
23.2
23.0

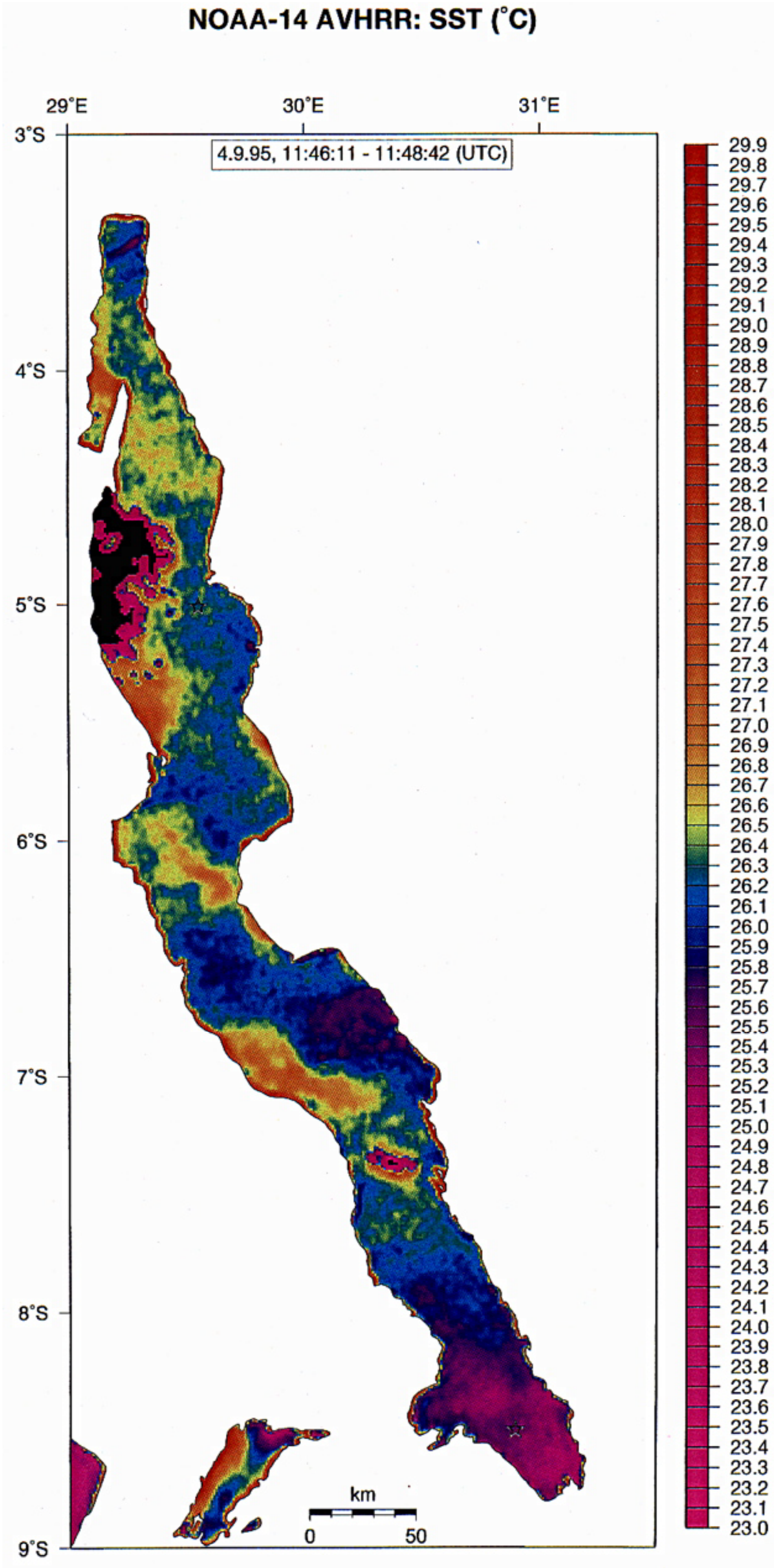
NOAA-14 AVHRR: SST (°C)
29°E
30°E
31°E
3°S
4°S
5°S
6°S
7°S
8°S
9°S
4.9.95, 11:46:11 - 11:48:42 (UTC)
km
0
50
29.9
29.8
29.7
29.6
29.5
29.4
29.3
29.2
29.1
29.0
28.9
28.8
28.7
28.6
28.5
28.4
28.3
28.2
28.1
28.0
27.9
27.8
27.7
27.6
27.5
27.4
27.3
27.2
27.1
27.0
26.9
26.8
26.7
26.6
26.5
26.4
26.3
26.2
26.1
26.0
25.9
25.8
25.7
25.6
25.5
25.4
25.3
25.2
25.1
25.0
24.9
24.8
24.7
24.6
24.5
24.4
24.3
24.2
24.1
24.0
23.9
23.8
23.7
23.6
23.5
23.4
23.3
23.2
23.1
23.0

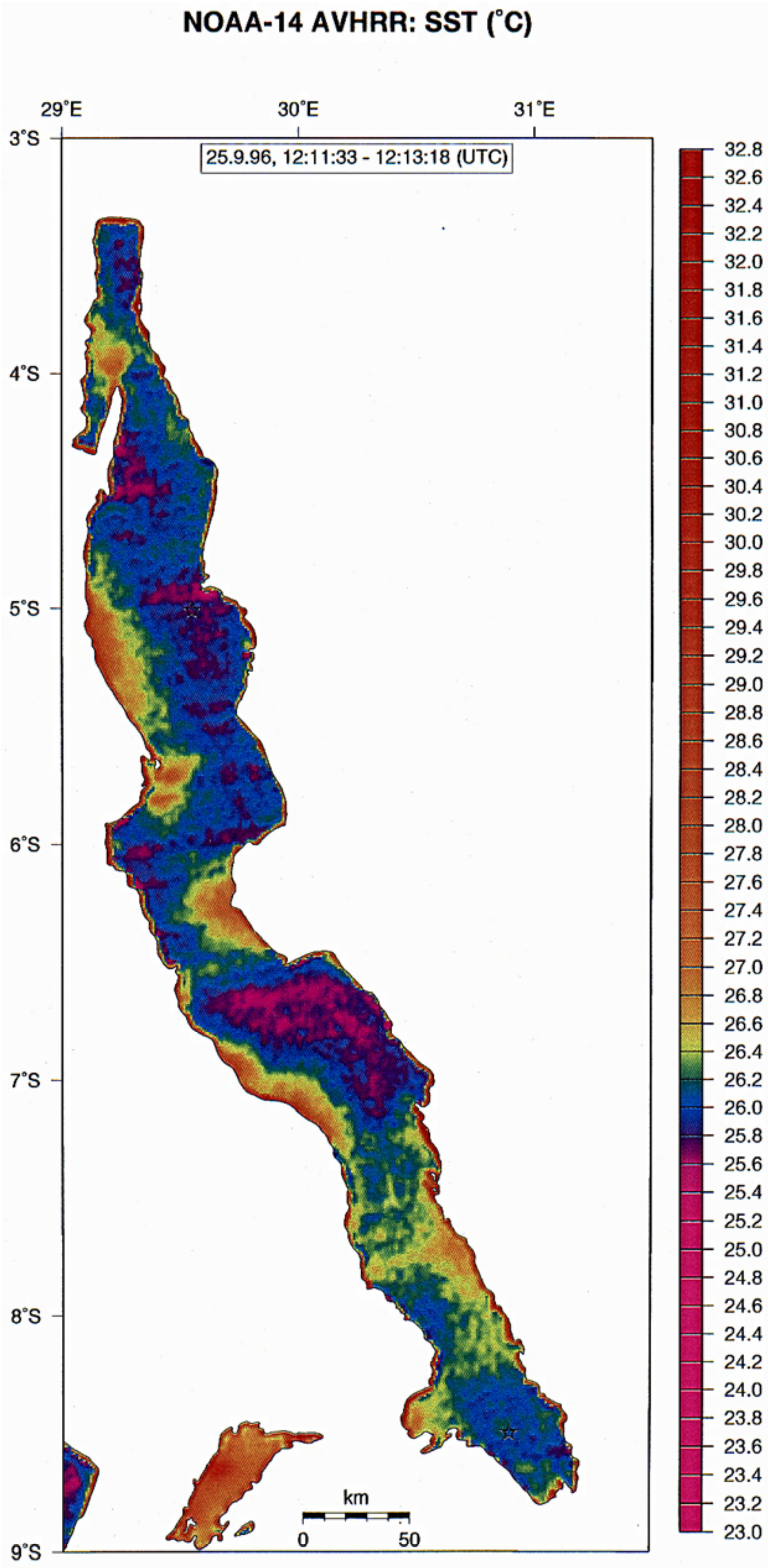
NOAA-14 AVHRR: SST (°C)
25.9.96, 12:11:33 - 12:13:18 (UTC)
29°E
30°E
31°E
3°S
4°S
5°S
6°S
7°S
8°S
9°S
km
0
50
32.8
32.6
32.4
32.2
32.0
31.8
31.6
31.4
31.2
31.0
30.8
30.6
30.4
30.2
30.0
29.8
29.6
29.4
29.2
29.0
28.8
28.6
28.4
28.2
28.0
27.8
27.6
27.4
27.2
27.0
26.8
26.6
26.4
26.2
26.0
25.8
25.6
25.4
25.2
25.0
24.8
24.6
24.4
24.2
24.0
23.8
23.6
23.4
23.2
23.0

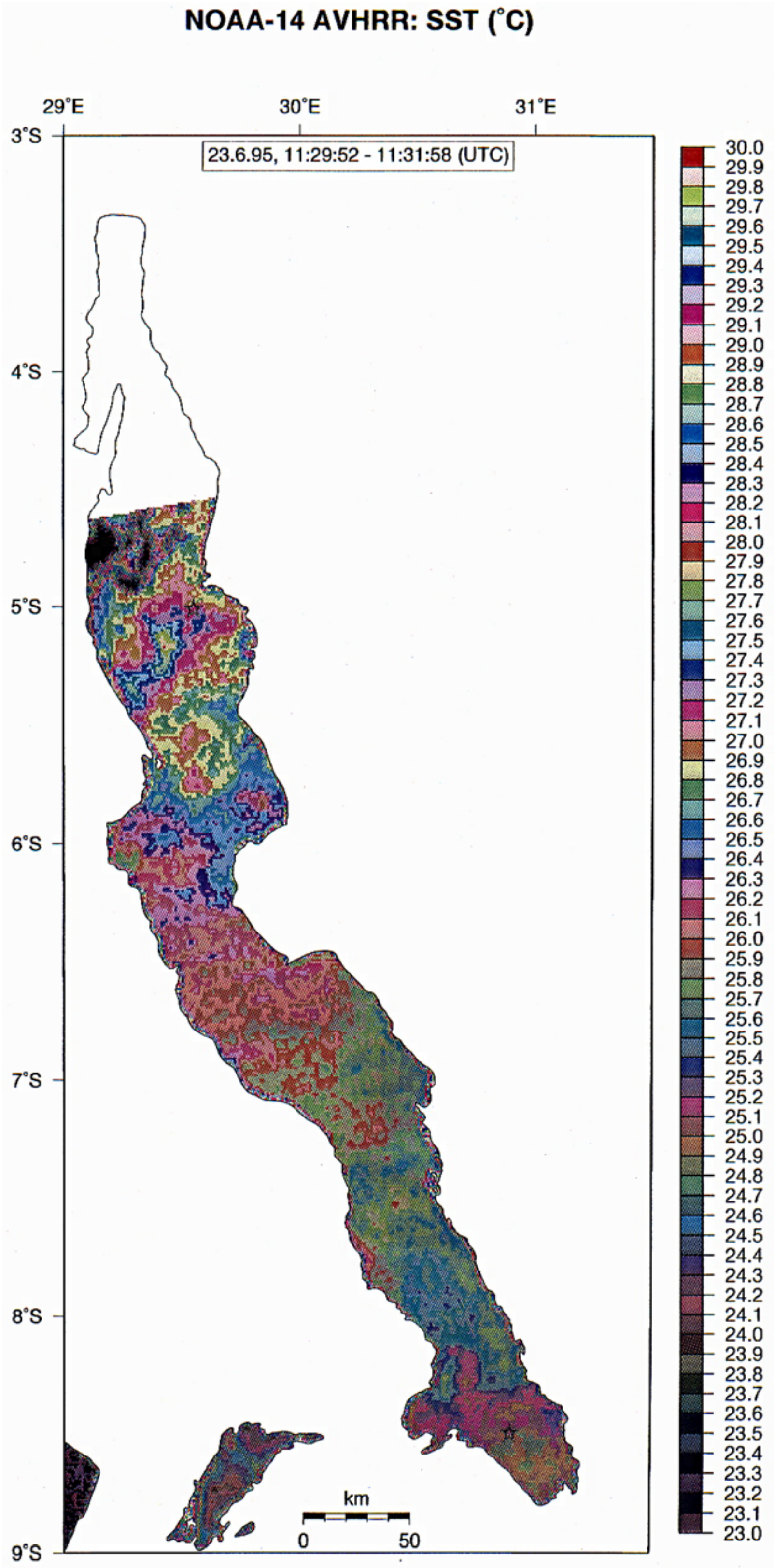
NOAA-14 AVHRR: SST (°C)
29°E
30°E
31°E
3°S
4°S
5°S
6°S
7°S
8°S
9°S
23.6.95, 11:29:52 - 11:31:58 (UTC)
km
0
50
30.0
29.9
29.8
29.7
29.6
29.5
29.4
29.3
29.2
29.1
29.0
28.9
28.8
28.7
28.6
28.5
28.4
28.3
28.2
28.1
28.0
27.9
27.8
27.7
27.6
27.5
27.4
27.3
27.2
27.1
27.0
26.9
26.8
26.7
26.6
26.5
26.4
26.3
26.2
26.1
26.0
25.9
25.8
25.7
25.6
25.5
25.4
25.3
25.2
25.1
25.0
24.9
24.8
24.7
24.6
24.5
24.4
24.3
24.2
24.1
24.0
23.9
23.8
23.7
23.6
23.5
23.4
23.3
23.2
23.1
23.0

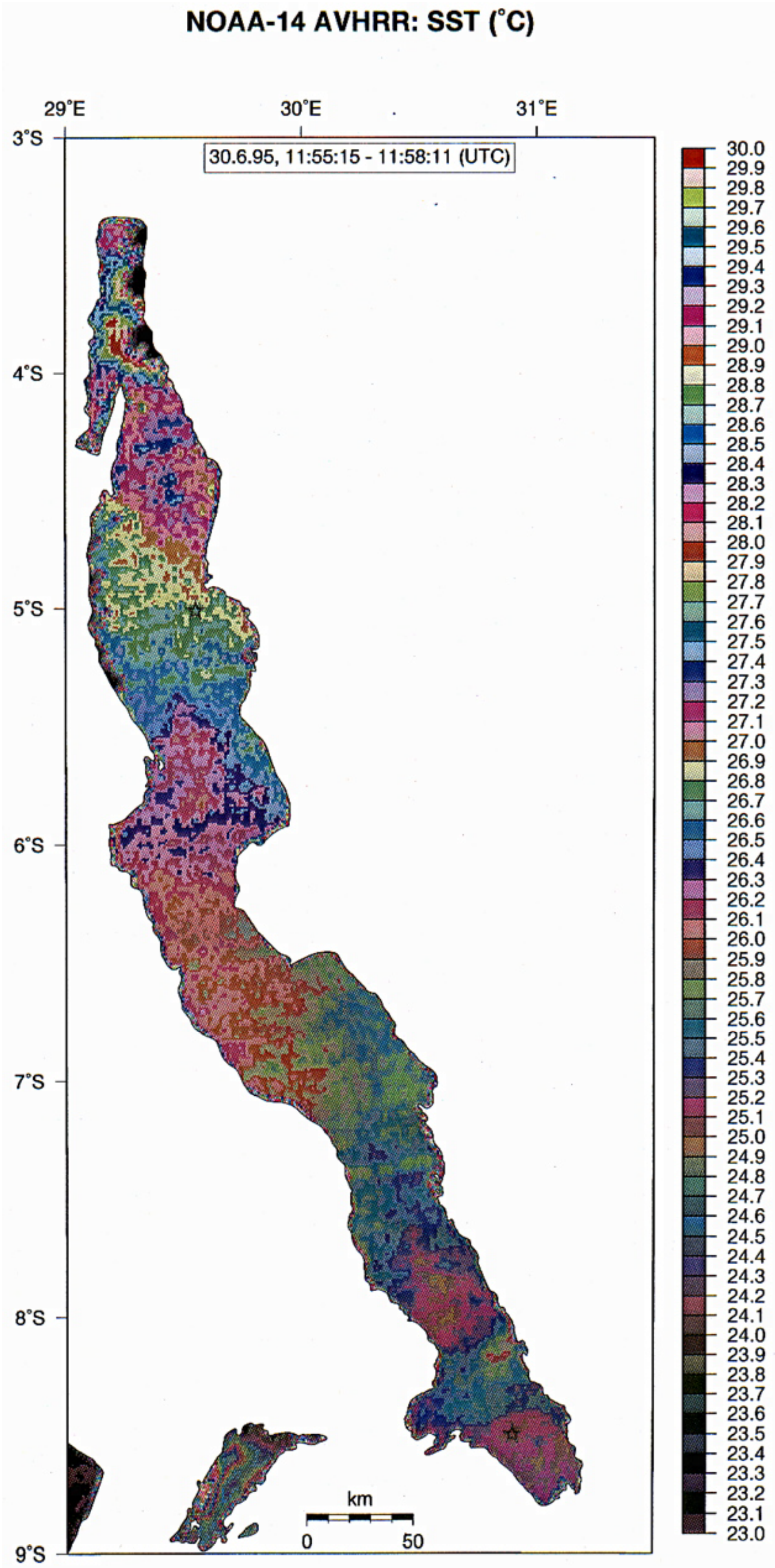
NOAA-14 AVHRR: SST (°C)
29°E
30°E
31°E
3°S
4°S
5°S
6°S
7°S
8°S
9°S
30.6.95, 11:55:15 - 11:58:11 (UTC)
km
0
50
30.0
29.9
29.8
29.7
29.6
29.5
29.4
29.3
29.2
29.1
29.0
28.9
28.8
28.7
28.6
28.5
28.4
28.3
28.2
28.1
28.0
27.9
27.8
27.7
27.6
27.5
27.4
27.3
27.2
27.1
27.0
26.9
26.8
26.7
26.6
26.5
26.4
26.3
26.2
26.1
26.0
25.9
25.8
25.7
25.6
25.5
25.4
25.3
25.2
25.1
25.0
24.9
24.8
24.7
24.6
24.5
24.4
24.3
24.2
24.1
24.0
23.9
23.8
23.7
23.6
23.5
23.4
23.3
23.2
23.1
23.0

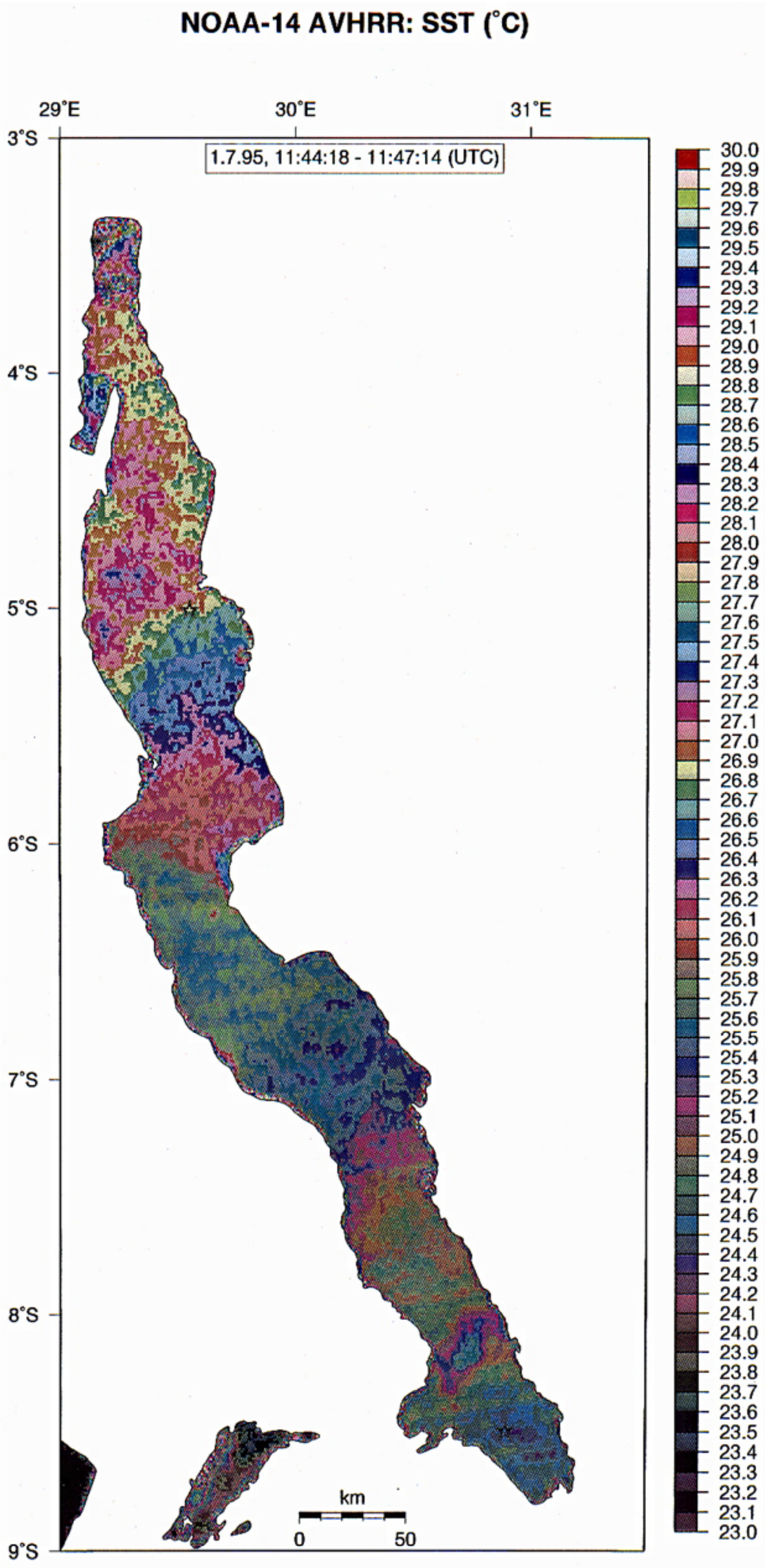
NOAA-14 AVHRR: SST (°C)
29°E
30°E
31°E
3°S
4°S
5°S
6°S
7°S
8°S
9°S
1.7.95, 11:44:18 - 11:47:14 (UTC)
km
0
50
30.0
29.9
29.8
29.7
29.6
29.5
29.4
29.3
29.2
29.1
29.0
28.9
28.8
28.7
28.6
28.5
28.4
28.3
28.2
28.1
28.0
27.9
27.8
27.7
27.6
27.5
27.4
27.3
27.2
27.1
27.0
26.9
26.8
26.7
26.6
26.5
26.4
26.3
26.2
26.1
26.0
25.9
25.8
25.7
25.6
25.5
25.4
25.3
25.2
25.1
25.0
24.9
24.8
24.7
24.6
24.5
24.4
24.3
24.2
24.1
24.0
23.9
23.8
23.7
23.6
23.5
23.4
23.3
23.2
23.1
23.0

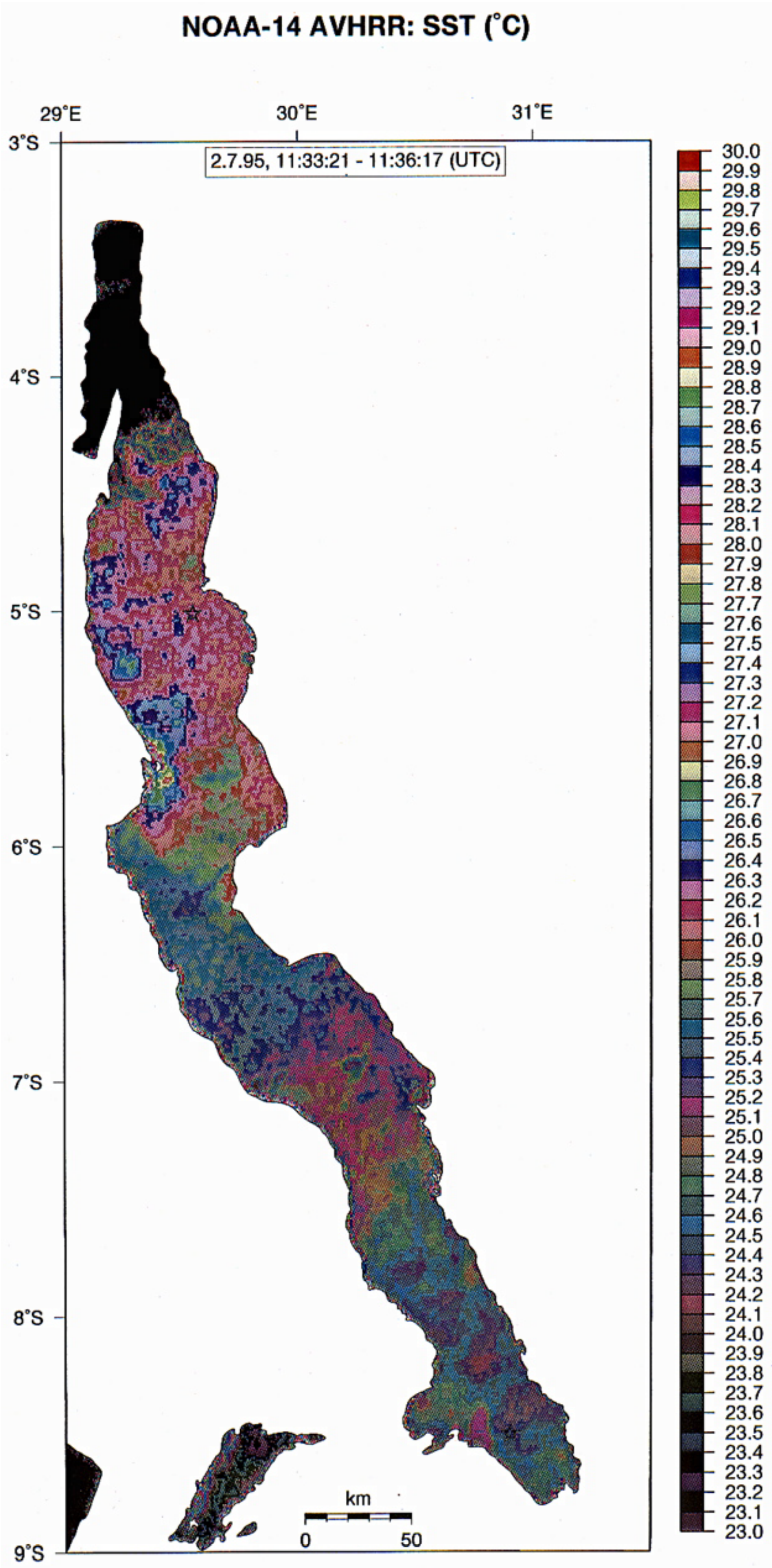
NOAA-14 AVHRR: SST (°C)
29°E
30°E
31°E
3°S
4°S
5°S
6°S
7°S
8°S
9°S
2.7.95, 11:33:21 - 11:36:17 (UTC)
km
0
50
30.0
29.9
29.8
29.7
29.6
29.5
29.4
29.3
29.2
29.1
29.0
28.9
28.8
28.7
28.6
28.5
28.4
28.3
28.2
28.1
28.0
27.9
27.8
27.7
27.6
27.5
27.4
27.3
27.2
27.1
27.0
26.9
26.8
26.7
26.6
26.5
26.4
26.3
26.2
26.1
26.0
25.9
25.8
25.7
25.6
25.5
25.4
25.3
25.2
25.1
25.0
24.9
24.8
24.7
24.6
24.5
24.4
24.3
24.2
24.1
24.0
23.9
23.8
23.7
23.6
23.5
23.4
23.3
23.2
23.1
23.0

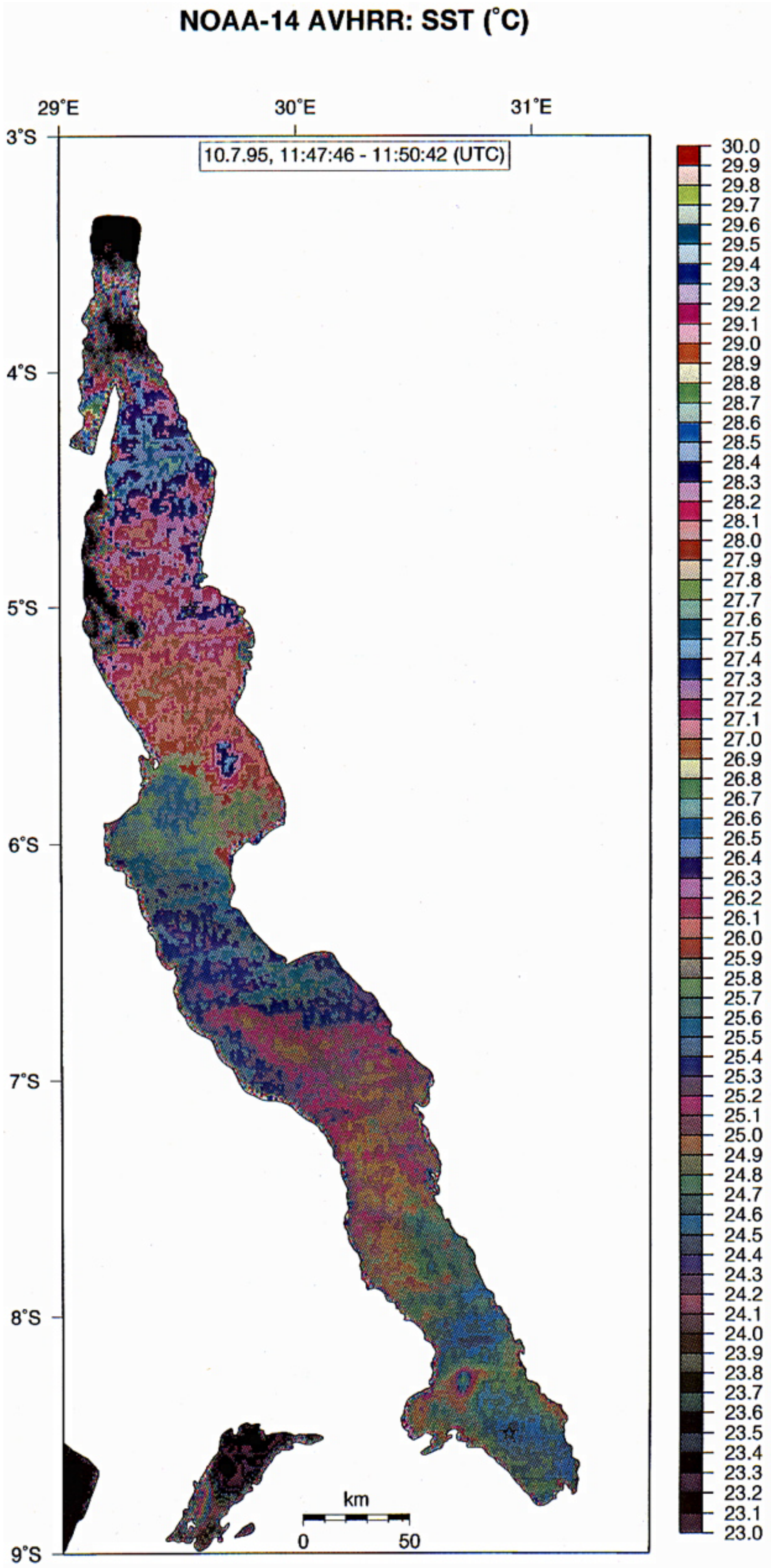
NOAA-14 AVHRR: SST (°C)
10.7.95, 11:47:46 - 11:50:42 (UTC)
29°E
30°E
31°E
3°S
4°S
5°S
6°S
7°S
8°S
9°S
km
0
50
30.0
29.9
29.8
29.7
29.6
29.5
29.4
29.3
29.2
29.1
29.0
28.9
28.8
28.7
28.6
28.5
28.4
28.3
28.2
28.1
28.0
27.9
27.8
27.7
27.6
27.5
27.4
27.3
27.2
27.1
27.0
26.9
26.8
26.7
26.6
26.5
26.4
26.3
26.2
26.1
26.0
25.9
25.8
25.7
25.6
25.5
25.4
25.3
25.2
25.1
25.0
24.9
24.8
24.7
24.6
24.5
24.4
24.3
24.2
24.1
24.0
23.9
23.8
23.7
23.6
23.5
23.4
23.3
23.2
23.1
23.0

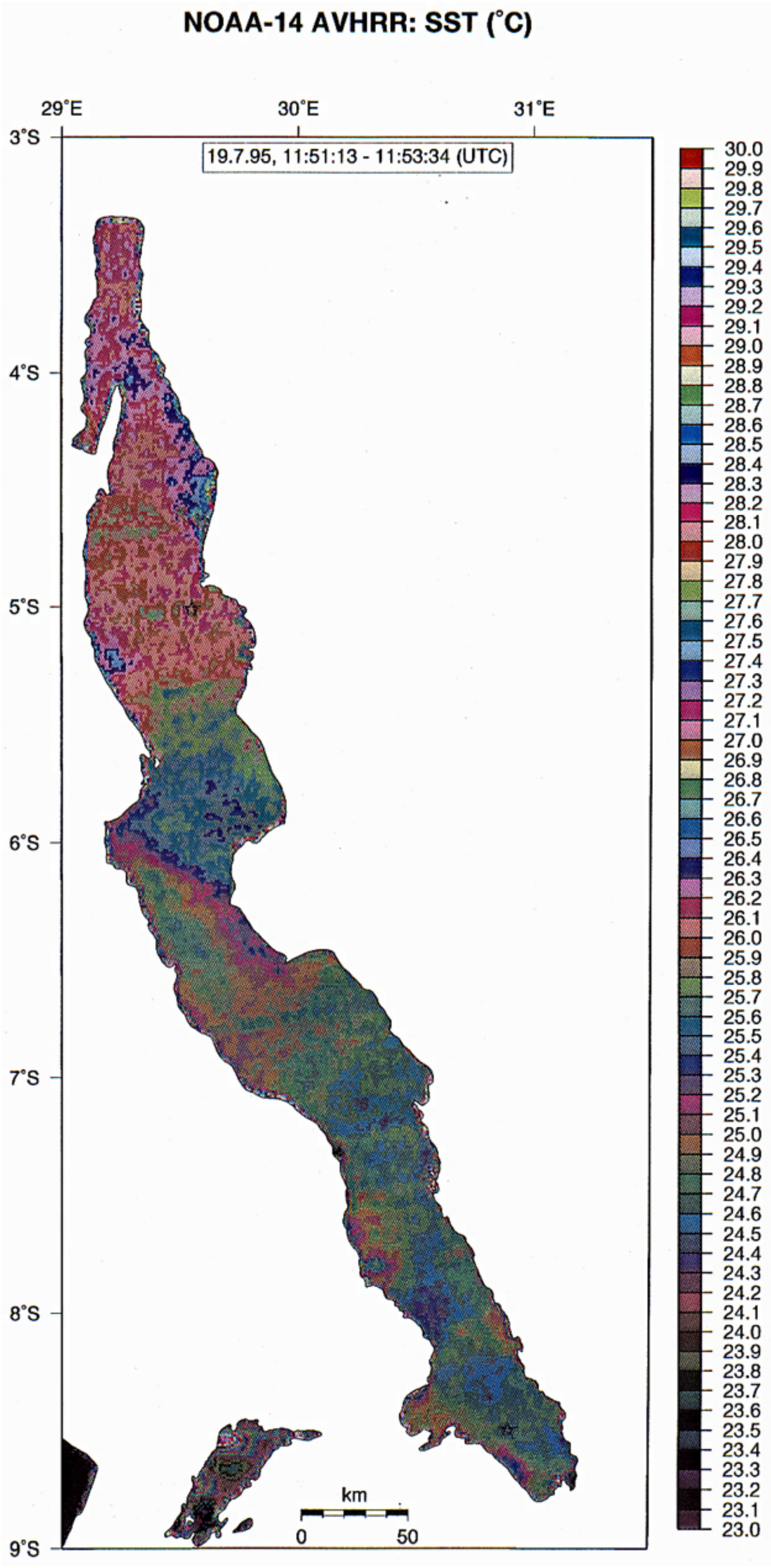
NOAA-14 AVHRR: SST (°C)
29°E
30°E
31°E
3°S
4°S
5°S
6°S
7°S
8°S
9°S
19.7.95, 11:51:13 - 11:53:34 (UTC)
km
0
50
30.0
29.9
29.8
29.7
29.6
29.5
29.4
29.3
29.2
29.1
29.0
28.9
28.8
28.7
28.6
28.5
28.4
28.3
28.2
28.1
28.0
27.9
27.8
27.7
27.6
27.5
27.4
27.3
27.2
27.1
27.0
26.9
26.8
26.7
26.6
26.5
26.4
26.3
26.2
26.1
26.0
25.9
25.8
25.7
25.6
25.5
25.4
25.3
25.2
25.1
25.0
24.9
24.8
24.7
24.6
24.5
24.4
24.3
24.2
24.1
24.0
23.9
23.8
23.7
23.6
23.5
23.4
23.3
23.2
23.1
23.0